

## Measurement of Vertebral Rotation from Moire Image for Screening of Adolescent Idiopathic Scoliosis

Ran CHOI<sup>†</sup>, Kota WATANABE<sup>‡</sup>, Nobuyuki FUJITA<sup>‡</sup>, Yoji OGURA<sup>‡</sup>, Morio MATSUMOTO<sup>‡</sup>, Satoru DEMURA<sup>††</sup>,  
Toshiaki KOTANI<sup>‡‡</sup>, Kanichiro WADA<sup>§</sup>, Masashi MIYAZAKI<sup>§§</sup>, Hideki SHIGEMATSU<sup>\*</sup>, Yoshimitsu AOKI<sup>†</sup> (*Member*)

<sup>†</sup> School of Science and Technology, Keio University, <sup>‡</sup> School of Medicine, Keio University

<sup>††</sup> Kanazawa University Hospital, <sup>‡‡</sup> Seirei Sakura Citizen Hospital, <sup>§</sup> Graduate School of Medicine, Hirosaki University

<sup>§§</sup> Oita University of Medicine, <sup>\*</sup> Nara Medical University

**<Summary>** Periodic spine screening in teenagers is important for early detection of adolescent idiopathic scoliosis, a deformity characterized by an abnormal spinal curve and vertebral rotation. Conventional methods for measuring vertebral rotation involve exposure to radiation and can be complicated by challenges inherent to manual identification of spinal features. We propose a method for automatic measurement of vertebral rotation using a nonradiation method that is easy to administer and is not associated with risk. To measure the angle of vertebral rotation from a Moire image, which is nonradiation method, convolutional neural network is applied to estimate the spinal position. In addition, to measure the angle from the spinal position in the transverse plane, we generate a spinal model of a teenager to obtain spinal dimensions in the transverse plane. The angle of vertebral rotation method is valid, having high correlation with method using computed tomography. The angle of vertebral rotation is meaningful for pathological diagnosis of adolescent idiopathic scoliosis.

**Keywords:** deep learning, spine estimation, vertebral rotation, spine screening

### 1. Introduction

Teenagers in an active growth stage require periodic spinal checkups for the early detection of adolescent idiopathic scoliosis (AIS), a structural scoliosis. This is because the curve of spine can progress rapidly during the growth stage, potentially becoming a serious disease. In addition, monitoring of curve progression is recommended for teens with mild AIS<sup>1)</sup>.

Structural scoliosis involves abnormal curvature and vertebral rotation (VR) of the spine and is caused by unknown factors. By contrast, a nonstructural scoliosis involves only spinal curvature and is a reversible condition caused by muscle spasms or differences in leg length. AIS is a structural scoliosis commonly diagnosed by measurement of the Cobb angle, an angle of abnormal spinal curvature<sup>2)</sup>. The Cobb angle is measured off the two-dimensional (2D) plane of a radiograph. Because it is difficult to measure VR radiographically, there exists no gold standard method for measuring VR.

Recently, methods for measuring VR have been reported<sup>3)</sup>.  
<sup>4)</sup> These methods were developed using imaging technologies and are based on an understanding of AIS as a three-dimensional (3D) deformity. VR can serve to diagnose AIS as

well as track spinal curve progression. Thus, VR is an indispensable means of diagnosing a pathological spinal condition<sup>5)</sup>. Current reported methods such as radiography and computed tomography (CT) involve exposure to radiation<sup>5), 6)</sup>. Consequently, these methods are not feasible for use as screening and monitoring tools for patients with AIS. Therefore, nonradiation methods for screening have been studied and developed. Unfortunately, mainly nonradiation methods measure surface metrics and not VR. These nonradiation methods are noninvasive and use optical measures of spinal curvature. These surface metrics generate other observations, such as imbalances of the trunk<sup>7)-10)</sup>. Treatment progress is evaluated based on the surface metrics of clinical deformity. However, these surface metrics are different from methods used in hospitals and have very little correlation to the Cobb angle<sup>6)</sup>. Back-surface curvature is a good descriptor of spinal shape, but this measure cannot explain the spinal condition, considering the structure of the spine itself.

Therefore, a screening method is needed that considers the spinal structure based on the surface of the back, does not involve radiation, and provides a pathological diagnosis by measuring VR. Given these needs, we propose a method for estimating spinal shape that measures VR based on surface

information. Furthermore, this method is designed to be automatic and not need any human interference.

As the back surface information, we use a Moire image which is broadly used in Japan and China (Hong Kong) for the early detection of AIS<sup>11)</sup>. We chose it due to the accumulated data by long period of use. This is an optical method as well as a surface descriptor like a contour line. About the evaluation indices of Moire method, description is in section 2. To estimate the spinal position from the Moire image, a convolutional neural network (CNN) is used. For the estimation of it using CNN, a dataset generation and CNN architecture are described in section 3. VR is an angle in the transverse plane ( $x, z$ ) whereas the estimated spinal position is 2D ( $x, y$ ) coordination. Accordingly, to measure the VR based on the estimated positions, we generate a general spinal model of teenagers to obtain the spinal dimensions to use instead of  $z$  coordination. A method measuring VR and the generation of general spinal model are explained in section 4. The validation of the method measuring VR and the result of estimation by CNN are described in section 5.

## 2. Related Methods and Their Evaluation Indices

Radiation methods used to diagnose AIS include radiography and CT; nonradiation methods use ultrasound, equipment, Moire, or smartphones.

The radiograph is the most commonly used 2D method for measuring the Cobb angle. On the radiographic image, the Cobb angle is obtained from the two most tilted vertebrae at both ends of one curve<sup>12)</sup>. Many methods exist to measure VR. The Perdriolle method is considered the most accurate and simplest to use and is based on the position of the pedicle and vertebral body, using a torsionmeter as in **Fig. 1** (a)<sup>5), 6)</sup>. Because these are manual measurements, observer errors exist. The observer error for the Cobb angle ranges from  $3^\circ$  to  $10^\circ$ . Furthermore, it is difficult to measure VR on radiographic images of poor clarity where feature identification is challenging<sup>5), 6)</sup>.

CT is a 3D method that reconstructs the spine using imaging techniques. From the 3D spine, the Cobb angle is measured on the coronal plane in a manner identical to how it is measured on a radiograph. According to the Ho method of measuring the VR on the CT, the most reliable and clinically useful method involves measuring the VR based on the vertical line and the bisecting line of the two lines connecting three features on the inner surface of the junction, as in **Fig. 1**(b). VR measurement is difficult because it requires identification of the apex of the vertebra from a 3D shape<sup>5), 6)</sup>.

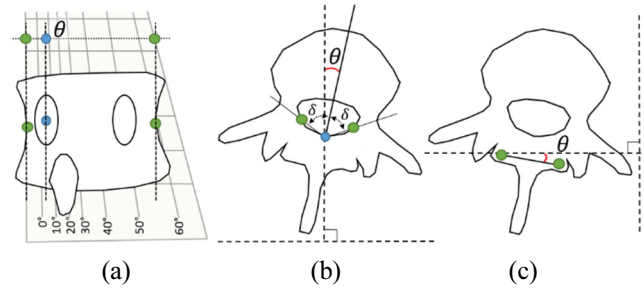


**Fig. 1** Methods for measuring VR; (a) radiography, (b) CT, and (c) ultrasound

Ultrasound does not involve radiation and is a 3D method that is easy to access in hospital settings. Instead of the Cobb angle, ultrasound measures the spinous process angle (SPA), which is highly correlated to the Cobb angle and uses the tips of the spinous process. The VR is an angle between the reference horizontal line and the line connecting the two laminae, as shown in **Fig. 1** (c). The lamina and the spinous process were identified manually on ultrasound images<sup>13), 14)</sup>.

Other nonradiation and optical methods exist, including the integrated shape imaging system, raster stereophotography, the quantec shape imaging system, and the formetric 3D. After attaching markers on anatomical landmarks, these techniques measure the back surface using the optical technology, producing descriptions of scoliosis based on surface matrices, such as shoulder, scapulae, and waist asymmetries, surface rotation, or trunk inclination on three planes: coronal, transverse, and sagittal<sup>7), 8), 15)</sup>. As we mentioned, surface metrics differ from indices such as the Cobb angle. For additional detail on these indices, please refer to Reference 7).

The Moire method is an optical method that describes the curvature and depth of the back surface, like a contour line. Using the Moire image, the spine can be classified as either normal or abnormal by manual scoring of the symmetry level by checking for equal depth. The Moire image shows the shape of the back but can be somewhat ambiguous in its interpretation. Notwithstanding, the Moire method is a costeffective and simple screening method<sup>7)-10)</sup>.

Kinect is a method that uses an RGB-D sensor for automatically estimating anatomical landmarks and spinal curve. This automated method for estimating landmarks replaces manual marking required during the use of optical methods<sup>16)</sup>. Kinect shows promise as a screening system that uses sensors instead of optical technology.

Additional smartphone applications<sup>17)</sup> that use a built-in gyro sensor, scolimeter, and scolioscreen exist. Such applications are easily accessed, requiring only downloading

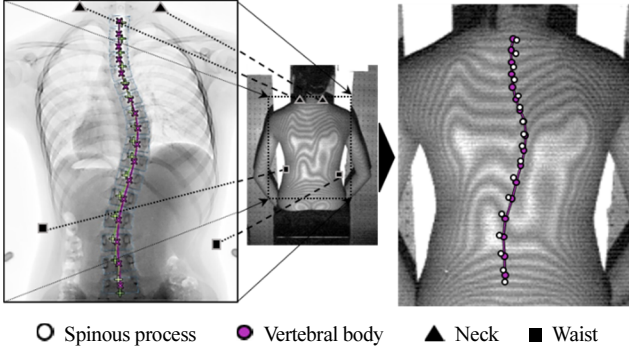


**Fig. 2** Dataset generated by merging the Moire image and spinal positions on radiography

of their application. Moreover, they are easy to operate, requiring the user to only drag the phone (supported by the thumbs) along the spinal curve. These applications can measure the angle of trunk rotation (ATR) in the Adams test position, similar to a scoliometer, which is a small tool for measuring ATR. This method does not require specific training; however, its accuracy is low because the ATR can be measured differently depending on the position of the thumbs or the phone.

We compared various spinal screening/diagnosis methods and evaluated the associated indices. Researches of measuring VR were reported only using radiation method and ultrasound method. The radiation-based methods are highly accurate but are associated with a high risk of radiation exposure. Nonradiation methods carry no risk of radiation, but they evaluate the spine using indices that cannot diagnose pathology and often require manual marking or identification of features.

### 3. Dataset and Spinal Estimation

#### 3.1 Dataset: Moire image and radiography

CNN used to estimate spinal positions from topography information called Moire. CNN is a technology for analyzing visual imagery and is used for detection or estimation in various fields<sup>18), 19)</sup>. To estimate the spine shape using CNN, a dataset is required that include Moire image with spine shape for training.

We collected 1965 pairs of Moire and radiographic images taken under different environments during the screening in their school and the diagnosis in the hospital respectively. Thus, a pose of subject was same standing upright in two images, but the poses were not exactly same because the images were taken in different time. We collected the data through Tokyo Health Service Association and the data was approved by the IRB. These data were obtained from

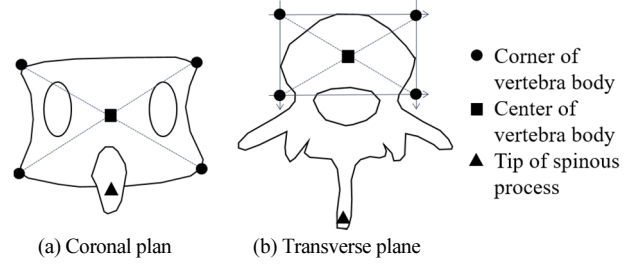


**Fig.3** Feature points in Coronal plane and Transverse plane

teenagers, aged 11–16 years, with Cobb angles ranging from  $0^\circ$  to  $55^\circ$ .

Because the Moire image includes back-surface information and the radiographic images include spinal information from the same subjects, we merged them into one dataset based on a silhouette and the points of neck and pelvis, as in **Fig. 2**. However, even if poses are exactly same, the body silhouettes of subject on two images were slightly different by the different view point between cameras. To minimize the difference, perspective projection was applied to merge two images. The mergence using the perspective projection was reported as a method has better estimation result by CNN than a mergence using translation and scaling. The mean absolute error (MAE) of spinal curve for each dataset was  $4.3^\circ$  for the dataset using perspective projection, and  $4.7^\circ$  for the dataset using translation and scaling<sup>20)</sup>. It means that the dataset merged by the perspective projection has higher accuracy because the estimation result will be better if the accuracy of dataset is higher. We used a dataset that was nearly identical to the dataset<sup>20)</sup>, but the dataset we used contained additional spinal feature, spinous process.

To verify the reproducibility of the dataset, one examiner merged 10 data twice on different days. The MAE of distance was small at  $3.9 \pm 2.6$  pixels. Therefore, a dataset which is similar to our dataset can be generated by others as well.

This spinal information comprised two features: a center of vertebral body and a tip of spinous process on one vertebra, as well as 12 thoracic (1T-12T) and 5 lumbar (1L-5L) vertebrae. We chose two features that are easily recognizable in radiographic image. In addition, the spinous process is a bone protruding from the vertebral body and is located the closest to the back surface, which is recognizable at back surface.

On the radiographic image, as shown in **Fig. 3** (a), the center of vertebral body is a gravity center point of four corners of vertebral body, and the tip of spinous process is the end point on a shape of spinous process. We divided the dataset into 200 data series for the test dataset and 1765 for the training dataset. The test dataset comprised 66 normal data series (Cobb angle  $< 10^\circ$ ), 70 data series with mild deformities ( $10^\circ \leq$  Cobb angle  $< 20^\circ$ ), and 64 data series with severe deformities ( $20^\circ \leq$  Cobb angle). To avoid overfitting problem

during the training, the training dataset augmented to 36652 by rotation ( $5^\circ$  clockwise and anti-clockwise) and mirroring. the end point on a shape of spinous process. We divided the dataset into 200 data series for the test dataset and 1765 for the end point on a shape of spinous process. We divided the dataset into 200 data series for the test dataset and 1765 for the training dataset. The test dataset comprised 66 normal data series (Cobb angle  $< 10^\circ$ ), 70 data series with mild deformities ( $10^\circ \leq$  Cobb angle  $< 20^\circ$ ), and 64 data series with severe deformities ( $20^\circ \leq$  Cobb angle). To avoid overfitting problem during the training, the training dataset augmented to 36652 by rotation ( $5^\circ$  clockwise and anti-clockwise) and mirroring.

### 3.2 Estimation of spine

We used AlexNet, which is a network architecture comprising five convolutional layers and two fully connected layers<sup>18), 19)</sup>. The architecture of the CNN is based on reference<sup>18)</sup>. The AlexNet is a relatively shallower network than other recent networks. We chose it because the mean absolute error (MAE) was the smallest. When we tested using same dataset described in section 3.1, the MAE of each network was  $3.89 \pm 1.98$  pixels for AlexNet,  $4.46 \pm 2.8$  pixels for VGGNet16<sup>21)</sup>, and  $4.1 \pm 2.5$  pixels for ResNet152<sup>22)</sup>. Deeper networks with more layers have more parameters that need to be optimized during the training. It requires bigger dataset for the difficult optimization<sup>22)</sup>. For this reason, it is assumed that the shallower network was effective at our small dataset rather than the deeper networks.

In CNN, the input was the Moire image and the output were 34 spinal positions of two features, a tips of spinous process and a center of vertebral body as shown in **Fig. 4**. These two kinds of feature were estimated using one network because they have a related structure. Before the Moire image was input into the CNN, the image was processed, the histogram was equalized to adjust the contrast, and a Fourier transformation was completed to remove noise. Appalment of Fourier transformation prevented the noise generated by rotating of Moire image for the data augmentation. The Fourier transformation removed low frequencies by masking using a  $100 \times 100$  rectangular window.

Afterward, the Moire image ( $640 \times 480$ ) was cropped based on spinal positions and then suitably resized for input ( $220 \times 220$ ) into the network.

## 4. Measurement of Vertebral Rotation

The vertebral rotation means a rotation in the vertebral axis. In this study, the angle of vertebral rotation (AVR,  $\theta$ ) is

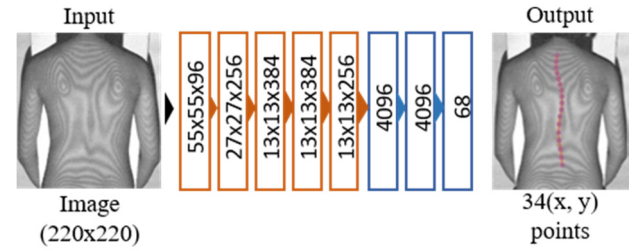


**Fig. 4** Architecture of CNN

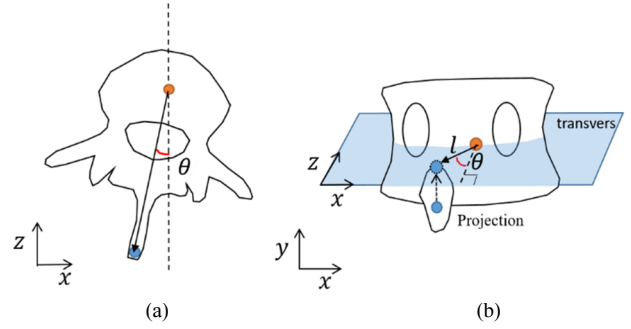


**Fig. 5** Transverse plane and coronal plan; (a) VR on the transverse plane which is the ground truth, (b) The proposed method for measuring AVR on the transverse plane using positions on the coronal plane

the angle formed by a vertical line and the line connecting the center of vertebral body and the tip of spinous process, on the transverse plane as shown in **Fig. 5** (a) where blue is the tip of the spinous process and orange is the center of the vertebral body. The vertical line was referenced from the coordinate on the data like Moire image or CT data.

We aimed at the AVR measurement from the estimated positions on the Moire image by CNN. However, the estimated positions included 2D ( $x, y$ ) data in the coronal plane and no ( $z$ ) depth, which was a necessary value for calculating AVR in the transverse plane. A general spinal dimension model is useful for referencing the distance between the center of vertebral body and the tip of spinous process. Thus, AVR was calculable using the length ( $L$ ) obtained from the spinal model, which is measured using a trigonometric function as shown in **Fig. 5** (b).

Since there exist no data pertaining to spinal dimensions in growing teenagers, we generated a general length model of spinal dimensions by annotating the features from CT data. The CT data were obtained from 20 teenagers (19 females, and 1 male) with severe AIS. The mean age of the teenagers was 15 years (range: 11- 19 years), weight was 44.2 kg (range: 33-56 kg), and height was 158 cm (range: 151.2-170.7 cm). The annotated data consisted of the center of the vertebral body and the tip of the spinous process.

On the CT image, the center of vertebral body was a gravity center point of four corners of vertebral body in both

planes, coronal and sagittal, and the tip of spinous process was the end point on a shape of spinous process in transvers plane (Fig. 3 (b)).

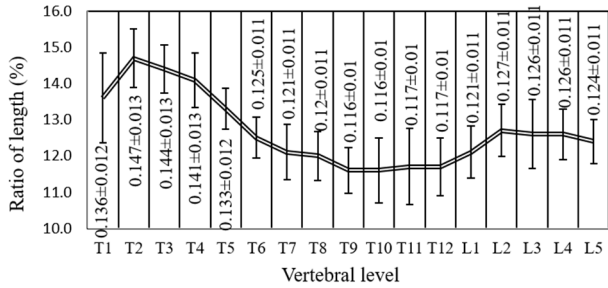


**Fig. 6** Spinal dimension of each vertebra based on the generated model

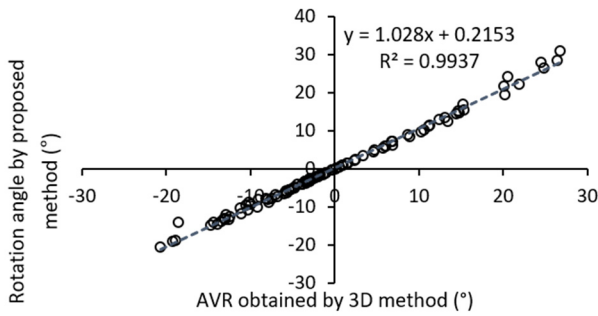


**Fig. 7** Correlation between the proposed method and 3D AVR method

**Table 1** MAEs of the proposed method and the ultrasound method

Range	MAE of proposed method	MAE of ultrasound <sup>13)</sup>
All	0.49° ± 0.81°	-
AVR  < 5°	0.11° ± 0.14°	0.3° ± 0.3°
5 ≤  AVR  < 10°	0.38° ± 0.46°	0.5° ± 0.3°
10 ≤  AVR  < 15°	0.51° ± 0.63°	1.0° ± 1.1°
15 ≤  AVR	1.76° ± 1.7°	-

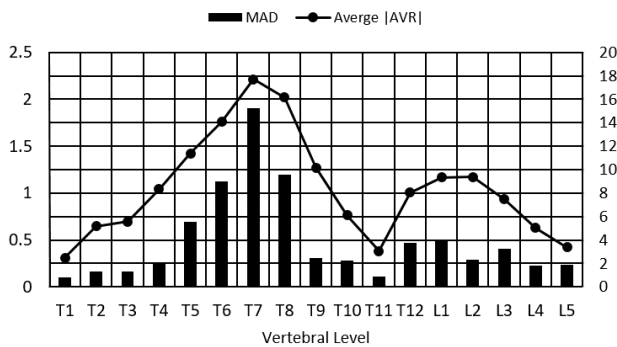


**Fig. 8** MAE and average |AVR| of each vertebral level

These data were normalized by dividing by the spinal length based on assumption that was made to establish the general model of spinal dimension (see Fig. 6). The assumption is that the length between the center of vertebra and the tip of spinous process is a function of spinal level and of spinal length<sup>15)</sup>. Figure 6 shows the spinal dimensions in ratio, which is the length, corresponding to each vertebral level.

The length ( $L$ ) indicates a length when the spinal length is 1; therefore,  $L$  was applied after conversion to an actual length multiplied by the spinal length. The spinal length was a length between two centers of vertebral bodies of T1 and L5.

AVR was calculated by  $\sin^{-1}(\Delta x/L)$ , and the programmed result was negative when the vertebra was twisted clockwise and positive when twisted counter-clockwise.

## 5. Experimental Results

### 5.1 Validation of AVR method

We compared our result to the ground truth. The ground truth was obtained by trigonometric function on feature points which were annotated from CT data by manually, as shown in Fig. 5 (a). The used dataset consisted of 6 females with severe AIS, aged 10-15, and mean height of dataset was 156 cm. The collected features were the tip of spinous process and the center of vertebral body. Our result was obtained by the proposed method based on the same data with the ground truth. The MAE for the entire vertebrae ( $n = 102, 6 \times 17$ ) was  $0.49^\circ \pm 0.81^\circ$ . The Pearson correlation coefficient ( $r$ ) of entire vertebrae was very high at 0.996 ( $p < 0.05$ ) and Fig. 7 shows the graph. The MAE of each AVR range, categorized by the angle obtained by the ground truth, were  $0.11^\circ \pm 0.14^\circ$ ,  $0.38^\circ \pm 0.46^\circ$ ,  $0.51^\circ \pm 0.63^\circ$  and  $1.76^\circ \pm 1.7^\circ$  for absolute AVR of  $0.0^\circ \sim 5.0^\circ$ ,  $5.0^\circ \sim 10.0^\circ$ ,  $10.0^\circ \sim 15.0^\circ$  and  $>15.0^\circ$  respectively, as shown in Table 1.

In addition, the MAE of ultrasound was reported that each MAE for absolute AVR of  $0.0^\circ \sim 5.0^\circ$ ,  $5.0^\circ \sim 10.0^\circ$  and  $10.0^\circ \sim 15.0^\circ$  were  $0.3^\circ \pm 0.3^\circ$ ,  $0.5^\circ \pm 0.3^\circ$  and  $1.0^\circ \pm 1.1^\circ$  respectively, as shown in Table 1. The ultrasound method measured the AVR as an angle between the reference horizontal line and the line connecting the two laminae, as shown in Fig. 1 (c). The ground truth was measured using MRI<sup>13)</sup>. In comparison with the MAE of ultrasound, the MAE of proposed method was smaller value in all absolute AVR ranges.

MAE and average absolute AVR of each vertebral level are shown in Fig. 8. In Fig.8, The average |AVR| is an average of two absolute values, which are the ground truth and the AVR



obtained by the proposed method. The vertebrae near neck (T1), pelvis (L5) and the part connected thoracic and lumbar vertebrae (T11 and T12), had smaller average absolute AVR, which means that deformity in the vertebra is small. This is inferred to be related to the usual shape of abnormal curve, which is C or S shaped and curved between two end vertebrae. Therefore, a vertebra such as T7, has high possibility to be located between the end vertebrae and vertebrae such as T1, T11 and L5 have high possibility to be the end vertebra.

Resultingly, both results in Table 1 and Fig.8 show that when absolute AVR is large, the MAE is large as well.

The Bland-Altman method was applied to access the agreement between the proposed method and the ground truth. Through the Bland-Altman, the difference between two methods can be analyzed<sup>23)</sup>. The average of the difference (bias) was  $-0.2$  and, the 95 % limits of agreement were  $1.72$  and  $-1.98$ . The Bland-Altman plot is shown in Fig.9.

Accordingly, our method is valid, having high correlation coefficient and small MAE with the ground truth. In addition, on analyzing the difference, MAE was larger when AVR was large.

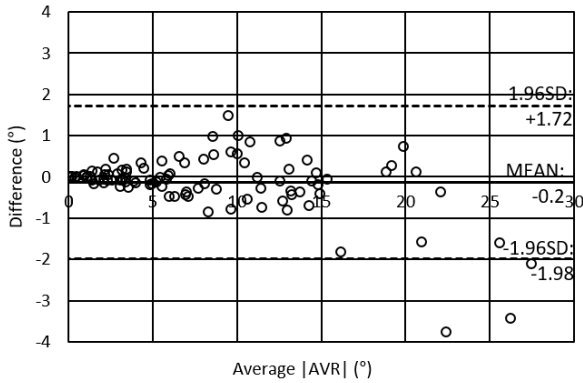


Fig. 9 Bland-Altman Plot

## 5.2 Estimation result and evaluation

CNN estimated the spine positions from the 200 Moire images in the test dataset. The ground truth was feature points on the Moire image. Both AVR of the ground truth and the estimation result were obtained by the proposed AVR method.

Figure 10 shows the spine and VR curves based on the ground truth and estimation result. On the center of back, the black line shows the spinal curve connecting the vertebral center, and the white line connects the spinous process and vertebral center on the same vertebral level. The orange line is the VR curve, indicating AVR calculated by the proposed method. The curve shapes on the ground truth and estimation result have similar curvature. Between the ground truth and the estimation result ( $n = 200 \times 34$ ), the MAE of distance was  $3.89 \pm 1.98$  pixels ( $6.8 \pm 3.6$  mm) in the Moire image.

In addition, using a method measuring Cobb angle (CA method), we evaluated the couverture of spinal curve, which is consisting of the center of vertebral body ( $n = 200$ ). The CA method was reported that has MAE of  $2.7^\circ$ <sup>20)</sup>. Cobb angles were measured based on the 17 centers of vertebral body, estimation result, and the maximum Cobb angle on the one spine compared with the Cobb angle measured on radiographic image by doctors. It is because doctors diagnose as AIS using the largest Cobb angle. The MAE were  $3.21^\circ \pm 2.2^\circ$  for normal (Cobb angle  $< 10^\circ$ ),  $4.7^\circ \pm 2.8^\circ$  for mild deformity ( $10^\circ \leq$  Cobb angle  $< 20^\circ$ ),  $7.3^\circ \pm 4.7^\circ$  for severe deformity ( $20^\circ \leq$  Cobb angle  $< 30^\circ$ ) and  $10.6^\circ \pm 5.0^\circ$  for severe deformity ( $30^\circ \leq$  Cobb angle  $\leq 45^\circ$ ), as shown in Table 2. Spine estimation had low accuracy when the deformity was severe.

Using the proposed AVR method, we measured AVR on the ground truth and estimation result ( $n = 200 \times 17$ ). MAE of

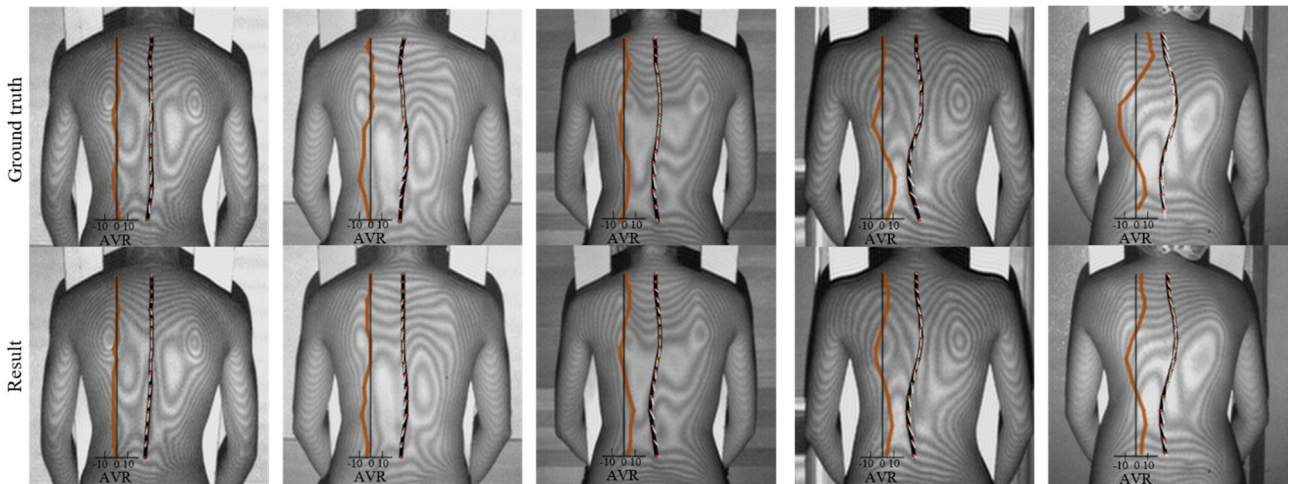
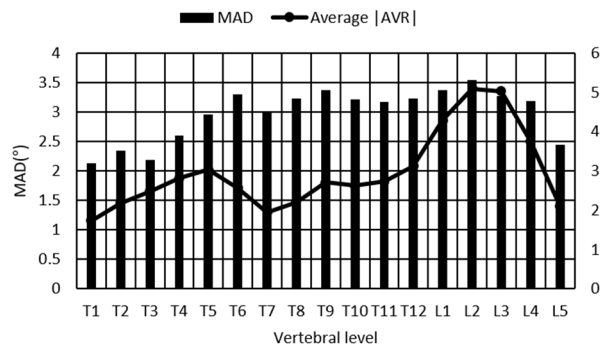


Fig. 10 Ground truth and estimation results

**Table 2** MAD of Cobb angle and MAD of absolute AVR between the estimation positions and the ground truth

Cobb angle	MAD	AVR	MAD
All	$6.0^\circ \pm 2.4^\circ$	All	$2.9^\circ \pm 1.4^\circ$
Cobb angle $< 10^\circ$	$3.21^\circ \pm 2.2^\circ$	$ AVR  < 5^\circ$	$2.0^\circ \pm 1.8^\circ$
$10^\circ \leq$ Cobb angle $< 20^\circ$	$4.7^\circ \pm 2.8^\circ$	$5^\circ \leq  AVR  < 10^\circ$	$4.3^\circ \pm 2.5^\circ$
$20^\circ \leq$ Cobb angle $< 30^\circ$	$7.3^\circ \pm 4.7^\circ$	$10^\circ \leq  AVR  < 15^\circ$	$6.5^\circ \pm 3.2^\circ$
$30^\circ \leq$ Cobb angle $\leq 45^\circ$	$10.6^\circ \pm 5.0^\circ$	$15^\circ \leq  AVR $	$12.7^\circ \pm 5.9^\circ$



**Fig. 11** MAD and average |AVR| of each vertebral level

AVR was  $2.9^\circ \pm 1.4^\circ$ . Each MAE for absolute AVR of  $0 \sim 5^\circ$ ,  $5^\circ \sim 10^\circ$ ,  $10^\circ \sim 15^\circ$ , and larger than  $15^\circ$ , were  $2.0^\circ \pm 1.8^\circ$ ,  $4.3^\circ \pm 2.5^\circ$ ,  $6.5^\circ \pm 3.2^\circ$  and  $12.7^\circ \pm 5.9^\circ$  respectively. **Figure 11** shows the MAE of AVR for each vertebral level. The MAE of AVR was larger when the deformity was severer, on the other hand, MAE was not large when average absolute AVR was large.

Consequently, on analyzing of the estimation result, Moire images with small deformity has more accurate result than Moire image with large deformity. The screening of AIS is targeted at classification into normal or mild eformity because severe deformity is recognizable in visually. Therefore, the proposed method measuring AVR on Moire image is able to support the screening of AIS.

## 6. Conclusion

We proposed a novel method for estimating spinal positions from a Moire image and measuring AVR, a crucial measure for diagnosing AIS.

An advantage of the proposed method is that the AVR is automatically measured only using the Moire image. This holds a considerable benefit considering the difficulties associated with measuring AVR by identifying spinal features. In this respect, our method is considerably different than the conventional method.

Although our nonradiation method used Moire images, we were able to diagnose the pathological condition in a manner similar to methods that use radiation. Consequently, our method is cost-effective and reduces the need for using radiation during screening. Screens that use nonradiation methods seek to classify those suspected of demonstrating AIS in order to refer these individuals to a hospital for additional diagnosis and treatment, if indicated. Historically, these methods identify many normal students because the classification scheme was based on surface metrics. Use of our method reduces the number of individuals suspected of demonstrating AIS by classification subdivision. Furthermore, our method is appropriate for monitoring by supplying the diagnostic index.

As a result, we supplied AVR angles. However, we cannot supply assessment results (normal or AIS). It is because the standard of AVR is not established yet. Accordingly, there is no clear AVR criteria for diagnosing AIS. Our results can be useful for establishing a VR standard and criteria for AVR.

## References

- 1) J. A. Janicki, B. Alman: "Scoliosis: Review of Diagnosis and Treatment", Paediatrics & Child Health, Vol. 12, No. 9, pp. 771–776 (2007).
- 2) J. D. Placzek, D. A. Boyce: The Spine, Elsevier, 3rd ed., pp. 470–473 (2016).
- 3) G. C. Lam, D. L. Hill, L. H. Le, J. V. Raso, E. H. Lou: "Vertebral Rotation Measurement: A Summary and Comparison of Common Radiographic and CT Methods", Scoliosis, Vol. 3, No. 16 (2008).
- 4) V. Pomerd, D. Mitton, S. Laporte, J. Guise, W. Skalli: "Fast Accurate Stereoradiographic 3D-Reconstruction of the Spine Using a Combined Geometric and Statistic Model", Clinical Biomechanics, Vol. 19, No. 3, pp. 240–247 (2004).
- 5) E. Ho, S. Upadhyay, F. Chan, L. Hsu, J. Leong: "New Methods of Measuring Vertebral Rotation from Computed Tomographic Scans: An Intraobserver and Interobserver Study on Girls with Scoliosis", Spine, Vol. 18, No. 9, pp. 1173–1177 (1993).
- 6) T. Vrtovec, F. Pernuš, B. Likar: "A Review of Methods for Quantitative Evaluation of Axial Vertebral Rotation", European Spine Journal, Vol. 18, No. 8, pp. 1079–1090 (2009).
- 7) P. Petros, T. B. Grivas, A. Kaspiris, C. Aggouris, E. Drakoutos; "A Review of the Trunk Surface Metrics Used as Scoliosis and Other Deformities Evaluation Indices", Scoliosis, Vol. 5, No. 12 (2010).
- 8) X.C. Liu, J.G. Thometz, J.C. Tassone, L.C. Paulsen, R.M. Lyon: "Historical Review and Experience with the Use of Surface Topographic Systems in Children with Idiopathic Scoliosis",

- International Conference on Information Systems (ISIS), Vol. 2, No. 8, pp.1–8 (2013).
- 9) H. Takasaki: “Moire Topography”, Applied Optics, Vol. 9 No. 6, pp.1467– 1472 (1970).
  - 10) M. Batouche: “A Knowledge Based System for Diagnosing Spinal Deformations: Moire Pattern Analysis and Interpretation”, Proc. of the 11th International Conference on Pattern Recognition, pp. 591–594 (1992).
  - 11) F. Altaf, J. Drinkwater, K. Phan, A.K. Cree: “Systematic Review of School Scoliosis Screening”, Spine Deformity, Vol. 5, No. 5, pp. 303–309 (2017).
  - 12) J.R. Cobb: “Outline for the Study of Scoliosis”, The American Academy of Orthopedic Surgeons Instructional Course Lectures, Vol. 5, pp. 261–275 (1948).
  - 13) Q. Wang, M. Li, E. H. M. Lou, W.C.W. Chu, M.S. Wong: “Validity Study of Vertebral Rotation Measurement Using 3-D Ultrasound in Adolescent Idiopathic Scoliosis”, Ultrasound in medicine & biology, Vol. 42, No. 7, pp. 1473–1481 (2016).
  - 14) M. L.M. Phil, J. Cheng, M. Ying, B. Ng, T. Lam, M. S. Wong: “A Preliminary Study of Estimation of Cobb's Angle from the Spinous Process Angle Using a Clinical Ultrasound Method”, Spine Deformity, Vol. 3, No.5, pp.476–482 (2015).
  - 15) D. Burkhard: “Rasterstereographic Measurement of Scoliotic Deformity”, Scoliosis, 9:22 (2014).
  - 16) V. Bonnet, T. Yamaguchi, A. Dupeyron, S. Andary, A. Seilles, P. Fraisse, G. Venture: “Automatic Estimate of Back Anatomical Landmarks and 3D Spine Curve from a Kinect Sensor”, Proc. of 2016 6th IEEE International Conference on Biomedical Robotics and Biomechatronics, pp. 924–929 (2016).
  - 17) O. I. Franko, C. Bray, P. o. Newton: “Validation of a Scoliometer Smartphone App to Assess Scoliosis”, Journal of Pediatric Orthopaedics, Vol. 32, No. 8, pp. e72–e75 (2012).
  - 18) A. Toshev, C. Szegedy: “DeepPose: Human Pose Estimation via Deep Neural Networks”, Proc. of The 2014 IEEE Conference on Computer Vision and Pattern Recognition, pp. 1654–1660 (2014).
  - 19) I. Goodfellow, Y. Bengio, A. Courville: Deep Learning, Available, <http://www.deeplearningbook.org/> (2016. Dec. 18), 1st ed., pp. 330–372 (2016).
  - 20) R. Choi, K. Watanabe, H. Jingui, N. Fujita, Y. Ogura, S. Demura, T. Kotani, K. Wada, M. Miyazaki, H. Shigematsu, Y. Aoki: “CNN-based Spine and Cobb Angle Estimator Using Moire Images”, IEEEJ Trans. on Image Electronics and Visual Computing, Vol. 5, No. 2, pp. 135–144 (2017).
  - 21) K. Simonyan, A. Zisserman: “Very Deep Convolutional Networks for Large-scale Image Recognition”, Proc. of International Conference on Learning Representation, arXiv: 1409.1556 (2015).
  - 22) K. He, X. Zhang, S. Ren, J. Sun: “Deep Residual Learning for Image Recognition”, Proc. of the IEEE Conference on Computer Vision and Pattern Recognition, pp. 770–778 (2016).
  - 23) D. Giavarina: “Understanding Bland Altman Analysis”, Biochemia Medica, Vol. 25, No. 2, pp. 141–151 (2015).

(Received Feb. 28, 2018)

(Revised Jun. 9, 2018)



#### **Ran CHOI**

She received her M.S. in Information science and Telecommunication from Hanshin University, Korea. She has received her Ph.D. in engineering from Keio University, Japan. Her research interests include medical imaging and computer vision.



#### **Kota WATANABE**

He received M.D. and Ph.D. from Keio University School of Medicine, Japan. He has been an assistant professor, with Department of Orthopedic Surgery, Keio University School of Medicine, Japan. Dr. Watanabe has received awards including The 35<sup>th</sup> Japanese Society for Spine Surgery and Related Research Taisho-Toyama Award, The 13<sup>th</sup> International Phillip Zorab Symposium Best Paper Award, and The 22nd International Meeting on Advanced Spine Techniques Whitecloud Award.



#### **Nobuyuki FUJITA**

He received M.D. and Ph.D. from Keio University School of Medicine, Japan. He is a board-certified orthopedic and spinal surgeon in Japan. He has been an assistant professor, with Department of Orthopedic Surgery, Keio University School of Medicine, Japan. He performs basic and clinical researches on spine.



#### **Yoji OGURA**

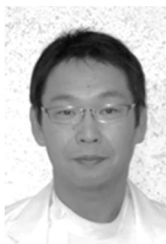
He received M.D. and Ph.D. from Keio University School of Medicine, Japan. He finished orthopaedic residency and spine surgery fellowship in Department of Orthopedic Surgery, Keio University school of Medicine, Japan. He had been a research fellow in RIKEN from 2012 to 2014. Since 2015, he has been an attending surgeon in Shizuoka Red Cross Hospital. Dr. Ogura has received awards including the 50th Scoliosis Research Society John H Moe Award, 29th Annual Research Meeting of Japanese Orthopaedic Association Best Presentation Award (second place) and 31st Annual Research Meeting of Japanese Orthopaedic Association Best Poster Award.





#### **Morio MATSUMOTO**

He received M.D. and Ph.D. from Keio University School of Medicine, Japan. Since 2015, He has been a chairman with Department of Orthopedic Surgery, Keio University school of Medicine, Japan.



#### **Satoru DEMURA**

He is an assistant professor, in the Department of Orthopedic Surgery, Kanazawa University, Japan. He received M.D. and Ph.D. from Kanazawa University School of Medicine, Japan. His main research includes treatment of spinal deformity, spine tumor and biomechanics of the spine.



#### **Toshiaki KOTANI**

He received M.D. and Ph.D. from Chiba University, School of Medicine, Japan. From 2010 to 2015, he was a director of spine center, Seirei Sakura Citizen Hospital, Japan. Since 2015, he has been a deputy director of Seirei Sakura Citizen Hospital, Japan. Dr. Kotani has received awards including Spinal Deformity Awards in 2003, 2004 and 2007.



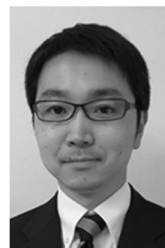
#### **Kanichiro WADA**

He received M.D. from Hirosaki University Graduate School of Medicine, Japan. He was an assistant professor with Department of Orthopaedic Surgery, Hirosaki University Graduate School of Medicine, Japan, from 2010 to 2013. Since 2014, He has been a lecturer, with Department of Orthopaedic Surgery, Hirosaki University Graduate School of Medicine, Japan. He performs researches in the clinical and epidemiological areas of spinal disorders.



#### **Masashi MIYAZAKI**

He received M.D. and Ph.D. from Oita University, School of Medicine, Japan. He is an assistant professor in Orthopaedic Surgery, Oita University Hospital, Oita, Japan. Dr. Miyazaki has received awards including 2008 North American Spine Society Outstanding Paper Award Runner-up and the 2nd Best Musculoskeletal Disease Paper Award.



#### **Hideki SHIGEMATSU**

He received M.D. and Ph.D. from Nara Medical University, Japan. He was a resident with Department of Orthopaedic Surgery, Tondabayashi Hospital, Japan, in 2000. He was a medical staff with Department of Orthopaedic Surgery, at Tondabayashi Hospital from 2001 to 2003, and Matsusaka Chuo Hospital from 2003 to 2005, and Yamatotakada municipal Hospital from 2009 to 2011 in Japan. He finished Fellowship in Hong Kong University. Since 2012, He has been an assistant professor with Department of Orthopaedic Surgery, Nara Medical University, Japan. Dr. Shigematsu is a member of Japanese Orthopaedic Association and Japanese Society for Spine Surgery and Related Research.



#### **Yoshimitsu AOKI** *(Member)*

He received his Ph.D. in Engineering from Waseda University in 2001. From 2002 to 2008, he was an associate professor, Department of Information Engineering, Shibaura Institute of Technology. Currently, he is a Professor, Department of Electronics & Electrical Engineering, Keio University. He performs researches in the areas of computer vision, pattern recognition, and media understanding.